Characteristic Flux-Difference Improvement for Inviscid and Viscous Hypersonic Blunt Body Flows

이 광섭, 홍 승규
국방과학연구소

Abstract

The Characteristic Flux Difference Splitting (CFDS) scheme designed to adapt the characteristic boundary conditions at the wall and inflow/outflow boundary planes satisfies Roe's property U, although the CFDS Jacobian matrix is decomposed by a product of elaborate transformation matrices and explicit eigenvalue matrix. When the CFDS algorithm, thus a variant of Roe's scheme, is applied straightforwardly to hypersonic flows over a blunt body, the strong bow shock gradually breaks down near the stagnation point. This numerical instability is widely observed by many researchers employing flux-difference method, known in the literature as the carbuncle phenomenon. Many remedies have been proposed and resulted in partial cures. When the idea of Sanders et al. which identifies the minimum eigenvalues near the discontinuity present is applied to CFDS method, it is shown that the instability problem can be controlled successfully. A few flux splitting methods have also been tested and results are compared against the Nakamori's Mach 8 blunt body flow.

1. Introduction

Pioneering works on CFD developments, especially at NASA-Ames along the line of flux-vector splitting methods[1-5] elevated potential and usefulness of CFD codes both as a design tool for future airplanes and as detailed flow simulations for phenomenological study. Lombard et al.[6-9] have also contributed their share in computing the Navier-Stokes equations through elaborate approaches which enable one to switch among the primitive, conservative and characteristic variable vectors easily and to apply the characteristic boundary conditions naturally. However, after much application of these schemes to complex flows with varying speeds and complexity, their weakness began to surface. For example, failure in capturing contact discontinuity, shock wave, and expansion wave with high

resolution and robustness is sometimes reported in resolving compressible flows. This is important especially for hypersonic flow computations where these waves become predominant. van Leer's flux-vector splitting (FVS) scheme[14] has shown the robustness for the strong normal shock and expansion waves. However, this scheme remained excessively dissipative for the contact discontinuity and the viscous regions. Nevertheless, the FVS scheme is quite effective for the computation of inviscid hypersonic flow because of its robustness for shock waves.

On the other hand, the flux difference splitting (FDS) such as Roe and CFDS are very accurate in the viscous region. But the FDS scheme produces nonphysical solutions when the grid is aligned with strong shock wave in hypersonic flow around a cylinder or spherical body. This is called the carbuncle phenomenon. Many researchers have observed this kind of shock instability when the shock and the grid become parallel to each other, making it look like a grid-aligned shock problem. The work of Quirk[10] is particularly enlightening on this aspect. The often-used remedy to cure the carbuncle flaw is via certain parameter-based switch in the regions where such phenomenon appear. It is observed[11] that the bow shock begins to break up when the magnitude of the velocity component parallel to the shock becomes zero. But the shock instability can be cured if we identify the eigenvalue corresponding to that velocity component and replace it which is nearly zero with other plausible values where necessary.

The objectives of present study are thus to revisit the carbuncle phenomenon which is especially paramount to Roe and CFDS schemes, to analyze its cause in terms of physical property changes across the shock and to offer possible remedy for the problem. The idea of Sander et al.[11] is incorporated into the CFDS method and is shown to provide a stable shock capture for the Mach 8 blunt body flow adapted as a benchmark case.

2. Numerical Method

The governing Navier-Stokes equations employed in the generalized coordinate system, (ξ, η, ϕ), are expressed for the conservative variable vector as

$$J^{-1}\frac{\partial q}{\partial t}+\frac{\partial}{\partial \xi}(\hat{F}+\hat{F}_v)+\frac{\partial}{\partial \eta}(\hat{G}+\hat{G}_v)+\frac{\partial}{\partial \phi}(\hat{H}+\hat{H}_v)=0 \qquad (1)$$

where $\hat{F}$, $\hat{G}$, and $\hat{H}$ are inviscid flux vectors, and $\hat{F}_v$, $\hat{G}_v$, $\hat{H}_v$ are viscous flux vectors. The inviscid fluxes are linearized and split for upwind

discretizations by

$$\triangle_\xi F = \hat{A}\triangle q = (\hat{A}^+ + \hat{A}^-)\triangle q \quad \text{and} \quad \hat{A}^\pm = \overline{M}\,\overline{T}\,\overline{\Lambda}^\pm\,\overline{T}^{-1}\,\overline{M}^{-1} \tag{2}$$

yielding

$$J^{-1}\delta q + \hat{A}^+\nabla_\xi q + \hat{A}^-\triangle_\xi q + \hat{B}^+\nabla_\eta q + \hat{B}^-\triangle_\eta q + \hat{C}^+\nabla_\phi q + \hat{C}^-\triangle_\phi q + (\text{viscous terms}) = 0 \tag{3}$$

where $\delta q = q^{n+1} - q^n$ and the overbar means the associated variable is space-averaged over the interval, [j, j+1]. $\overline{M}$ or $\overline{M}^{-1}$ is a transformation matrix between the conservative variable vector q and the primitive variable vector, say, $\tilde{q}$. $\overline{T}$ or $\overline{T}^{-1}$ is defined to be a transformation matrix between the primitive variable vector $\tilde{q}$ and the characteristic variable vector, say, $\tilde{\tilde{q}}$.

The formulation procedure can be summarized as follows: i) $\triangle F$ known, ii) $\triangle q$, $\triangle\tilde{q}$ defined iii) $\overline{M}$, $\overline{M}^{-1}$ determined from $\triangle\tilde{q} = \overline{M}^{-1}\triangle q$, iv) $\overline{A}$ determined from $\overline{A}\triangle\tilde{q} = \overline{M}^{-1}\triangle F$, v) $\overline{\Lambda}$ known/satisfies $|\overline{\Lambda} - \overline{A}| = 0$, vi) $\overline{T}^{-1}\overline{A} = \overline{\Lambda}\,\overline{T}^{-1}$ determines $\overline{T}^{-1}$ or $\overline{T}$.

The strength of current formulation, termed as Characteristic Flux Difference Splitting (CFDS) scheme, is to enable one to switch the difference equation from the conservation form

$$\frac{J}{\Delta t}\delta q + \overline{M}\,\overline{T}\,\overline{\Lambda}\,\overline{T}^{-1}\,\overline{M}^{-1}\Delta q = 0 \tag{4}$$

to characteristic form

$$\frac{J}{\Delta t}\delta\tilde{\tilde{q}} + \overline{\Lambda}\Delta\tilde{\tilde{q}} = 0 \tag{5}$$

rather easily written for one-dimensional case for the sake of simplicity. Details of the formulation and its applicability to characteristic boundary procedure are given in Ref. 12.

When the eigenvalue becomes zero in Eq. (5), there is no convective wave information traveling to that point as occurs in the stagnation line. Since the CFDS formulation also splits the eigenvalue as

$$\Lambda = \Lambda^+ + \Lambda^- \tag{6}$$

this splitting is also susceptible to carbuncle problem when λ_1 becomes zero. When the velocity component parallel to the shock becomes zero, the associated eigenvalue matrix becomes

$$\overline{\Lambda} \cong \begin{bmatrix} u & & & & \\ & u & & & \\ & & u & & \\ & & & u+c & \\ & & & & u-c \end{bmatrix} = \begin{bmatrix} 0 & & & & \\ & 0 & & & \\ & & 0 & & \\ & & & c & \\ & & & & -c \end{bmatrix} \tag{7}$$

Thus it is necessary to prevent the eigenvalue component from becoming zero. This can be done via

$$\lambda = \lambda^+ + \lambda^- = (\lambda^+ + \varepsilon) + (\lambda^- - \varepsilon) \tag{8}$$

with a proper choice of ε. Sanders et al[11] recently finds the H-correction method work well preventing the bow shock instability via

$$\lambda^H{}_{j+1/2,k} = \max(\lambda_{j+1/2,k}, \lambda_{j,k+1/2}, \lambda_{j,k-1/2}, \lambda_{j+1,k+1}, \lambda_{j+1,k-1/2}).$$

On the other hand, the entropy fixing method proposed by Harten[15] and its variants can eliminate the shock instability problem. But this method is advisable only for the strong shock flows since this injects excessive numerical dissipation in the viscous region. Quirk also provides a convenient way of checking the occurrence of shock from a pressure ratio test $\frac{|P_R - P_L|}{\min(P_L, P_R)} > \alpha$, where $\alpha = 20$ is used for the present study. In the present study for blunt body flow calculations, the entropy fixing formula employed are

i) for the Roe scheme

$$|\lambda| = \left(\frac{\lambda^2 + \varepsilon^2}{2\varepsilon}\right) \quad \text{if } |\lambda| < \varepsilon, \text{ and} \tag{9}$$

ii) for the CFDS scheme

$$|\lambda| = \left(\frac{\lambda^2 + \varepsilon^2}{2\varepsilon}\right) * sign(\lambda) \quad \text{if } |\lambda| < \varepsilon \tag{10}$$

with $\varepsilon = 2.0$.

3. Numerical Experiments

An example case is run for a hypersonic flow past a cylinder at Mach 8 with α=0. The same flow was investigated by Nakamori[13] in conjunction with overcoming the carbuncle phenomenon. It is thus our purpose to compare present results with those of Ref. 13 and to see if the proposed modification we are incorporating work well in light of the known results. The computational grid as shown in Fig. 1 consists of 101x50 for (ξ, η). Figure 2 shows the blunt body flow using van Leer's FVS scheme for the Euler equation with CFL number of 0.6 which is free from carbuncle

phenomenon. Mach and pressure contours are shown in Fig. 2, exhibiting a strong bow shock in front of the body. Distributions of pressure, density, and temperature along the stagnation line are also presented in Fig. 2(c) showing a stiff jump across the shock layer. Euler equation is integrated by four-step Runge-Kutta method. In contrast, as shown in Fig. 3, the Roe scheme suffers from the serious carbuncle phenomenon. The stagnation properties are also poorly calculated showing breakdown of the shock formation. However, Fig. 4 shows a stable capture of the shock with the Roe scheme where the physical variables show a perfect match between those in Fig. 2(c) and in Fig. 4(c) after utilizing the λ fix given in Eq. (9) above. However, temperature and density profiles near the wall, x=0, display slight tail-off or tail-up compared to the van Leer's results. This is probably due to insufficient number of iterations in the Roe case, showing a slower convergence near the wall.

The same problem was solved by the present CFDS scheme with first order DDADI integration method and characteristic boundary conditions. Figure 5 contains Mach and pressure contours as well as stagnation line properties. Being a variant of Roe-type scheme, the unmodified CFDS also yields carbuncle problem as was observed by the Roe scheme without λ modification. After utilizing the λ modification as given in Eq. (10) above, stable results are obtained as shown in Fig. 6 in terms of the same quantities which compare well with those obtained earlier in Figs. 2 and 4. Comparison of the λ_1 distribution is given in Fig. 7 between the original λ_1 and the modified λ_1, showing a monotonic variation of original λ_1 and a sudden jump of λ_1 in the modified case. The modified λ_1 curve is similar to van Leer's flux variations against Mach number value[16]. In Fig. 7, the grid point j=51 corresponds to the stagnation line, but the value of λ_1 changes its sign at the interval [50,51] due to the averaged nature of flux-difference formulation.

Other physical variables are also compared in Fig. 8 along the stagnation line between the original λ_1 and the modified λ_1 cases in terms of entropy change, total enthalpy and the u-velocity. In the numerically unstable case, the entropy decreases and the u-velocity component becomes negative across the shock layer. On the other hand, for the λ-modified case the total enthalpy shows no change, the entropy increases and the

u-velocity decreases but maintains the positive sign as in Fig. 8(b). Figure 9 displays the velocity vector plots near the distorted shock region in Fig. 9(a) and the well-behaved velocity vectors in Fig. 9.(b). It shows the presence of big circulation behind the shock with the reverse u-velocity which becomes larger and larger as the iteration proceeds. The cause of this carbuncle phenomenon is believed to stem from the λ splitting $\lambda=\lambda^{+}+\lambda^{-}$ according to the sign of λ. When λ=0, the convective part of flux disappears feeding unphysical flux into the system.

Concluding Remarks:

The carbuncle phenomenon has been investigated in the CFDS framework. The CFDS being a flux-difference family also suffers from shock instability problem. To circumvent this, Sanders-type λ modifications have been applied among currently available λ fixes reported in the literature. The success with Sanders-type λ fix applied to the CFDS enables one to apply the CFDS method to a more wide range of flows with speed and complexity, resulting in remarkably improved solutions, for example, for a complex jet impingement problem within a confined geometry. However, it remains to prove that the current type of λ fix is really universal to warrant a permanent CFDS correction.

References

1. Warming, R.F. and Beam, R. M.,"On the Construction of Implicit Factored Schemes for Conservation Laws," Computational Fluid Dynamics, SIAM-AMS Proceedings, Vol. 11, 1978, pp.85-127.

2. Pulliam, T. H. and Steger, J. L. "On Implicit Finite Difference Simulations of Three-Dimensional Flows," AIAA-78-10, January 1978.

3. Steger, J. L. and Warming, R. F., "Flux Vector Splitting of the Inviscid Gasdynamic Equations with Application to Finite Difference Methods," J. Comp. Phys., Vol. 40., No.2, 1981, pp. 263-293.

4. Pulliam, T. H. and Chaussee, D. S., "A Diagonal Form of an Implicit Approximate-Factorization Algorithm,", Journal of Computational Physics, Vol. 39, pp.347-363, 1981.

5. Steger, J. L. "The Chimera Method of Flow Simulation," Workshop on Applied Computational Fluid Dynamics, August 1991.

6. Lombard, C. K., Oliger, J., Yang, J. Y. and Davy, W. C., "Conservative Supra-Characteristics Method for Splitting the Hyperbolic Systems of Gasdynamics with Computed Boundaries for Real and Perfect Gases," AIAA-82-0837, June 1982.

7. Lombard, C. K., Oliger, J., Yang, J. Y. "A Natural Conservative Flux Difference Splitting for the Hyperbolic Systems of Gasdynamics," AIAA-82-0976, June 1982.

8. Lombard, C. K., et al., "Multi-Dimensional Formulation of CSCM - An Upwind Flux Difference Eigenvector Split Method for the Compressible Navier-Stokes Equations", AIAA-83-1895, AIAA 6th CFD Conference, July 1983.

9. Hong, S. K., Bardina, J., Lombard, C. K., Wang, D. and Codding, W., "A Matrix of 3-D Turbulent CFD Solutions for JI Control with Interacting Lateral and Attitude Thrusters,"AIAA 91-2099, Sacramento, June 1991.

10. Quirk, J. J., "A Contribution to the Great Riemann Solver Debate," Intl. J. for Numerical Methods in Fluids, Vol. 18, pp. 555-574, 1994.

11. Richard Sanders, E. Morano, and M.C. Rduguert, "Multidimensional Dissipation for Upwind Schemes: Stability and Applications to Gas Dynamics," J. of Computational Physics. 145, 511-537(1998).

12. 홍승규, 이광섭,"Application of Characteristic Boundary Conditions in the Flux-Difference Splitting Framework," 대한기계학회 '99년도 유체공학부문 춘계학술강연회 강연집, pp.141-156, 한양대학교, 1999. 5.

13. I. Nakamori and Y. Nakamura, "An Upwind Scheme for Inviscid and Viscous Hypersonic Flow," AIAA-95-1732-CP.

14. Roe, P. L., "Approximate Riemann Solvers, Parameter Vectors, and Difference Schemes," J. of Computational Physics 43, 1981, pp. 357-372.

15. A. Harten, "High Resolution Schemes for Hyperbolic Conservation Laws," J. of Computational Physics, Vol. 49, 1983, pp. 357-393.

16 C. Hirsch, "Numerical Computation of Internal and External Flows," John Wiley & Sons, 1988.

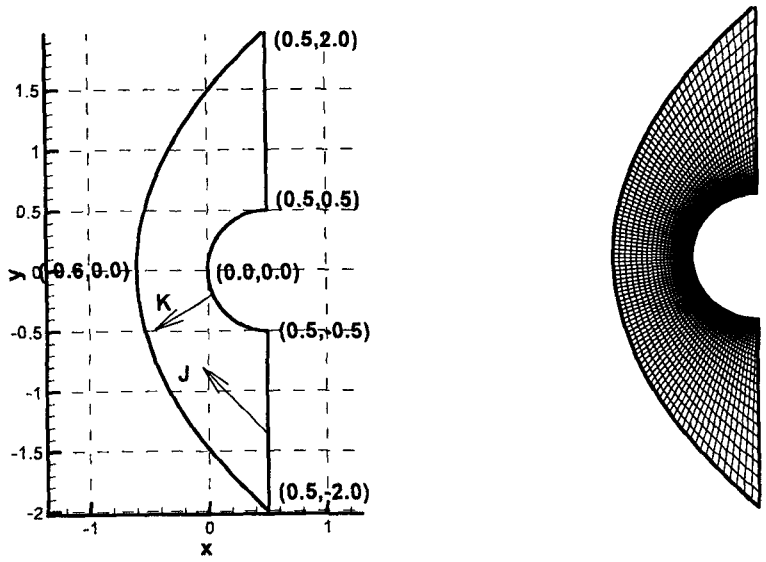

Figure 1. Grid system of a cylinder(101X50 mesh)

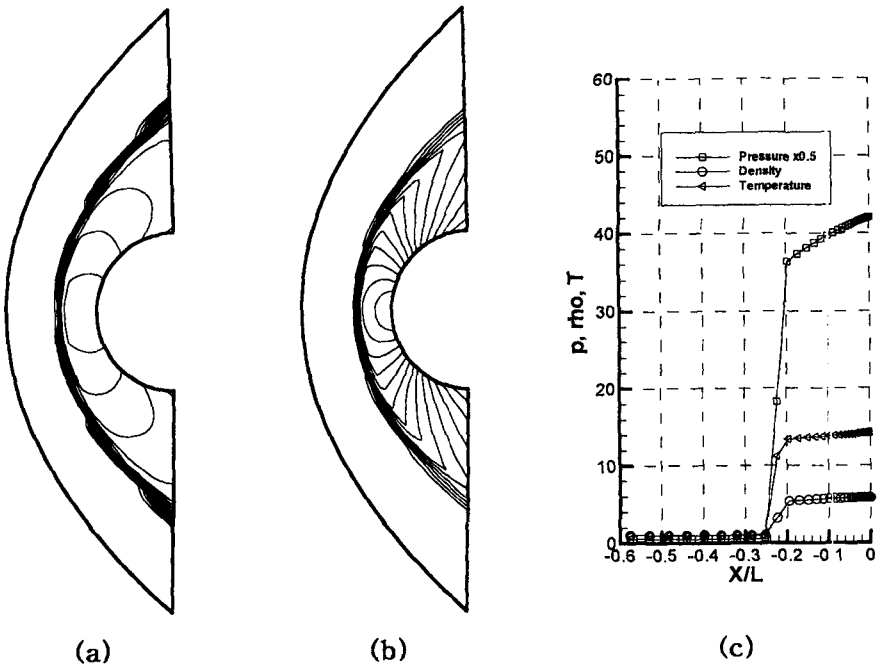

(a) (b) (c)

Figure 2. Hypersonic flow solved by the van Leer scheme at Mach 8
(a) Mach contours; (b) Pressure contours; (c) Stagnation line properties

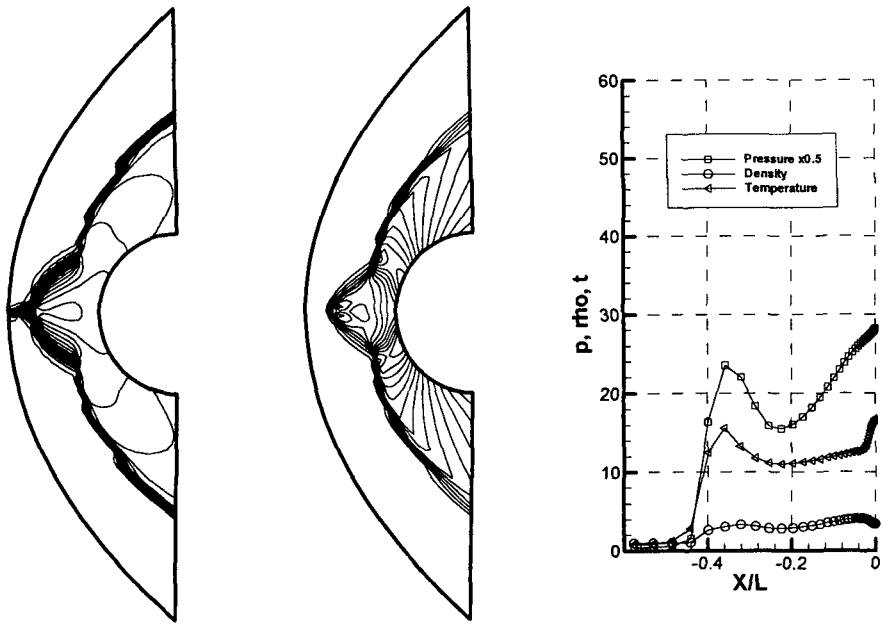

(a) (b) (c)

Figure 3. Hypersonic flow solved by the Roe scheme at Mach number of 8
(a) Mach contours; (b) Pressure contours; (c) Stagnation line properties

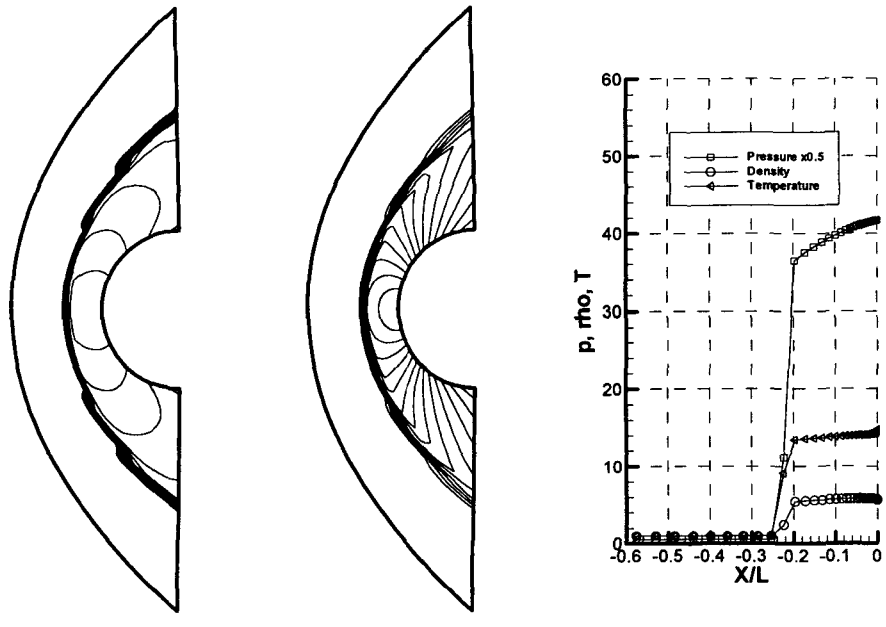

(a) (b) (c)

Figure 4. Hypersonic flow solved by the Roe scheme (eigenvalue modified)
(a) Mach contours; (b) Pressure contours; (c) Stagnation line properties

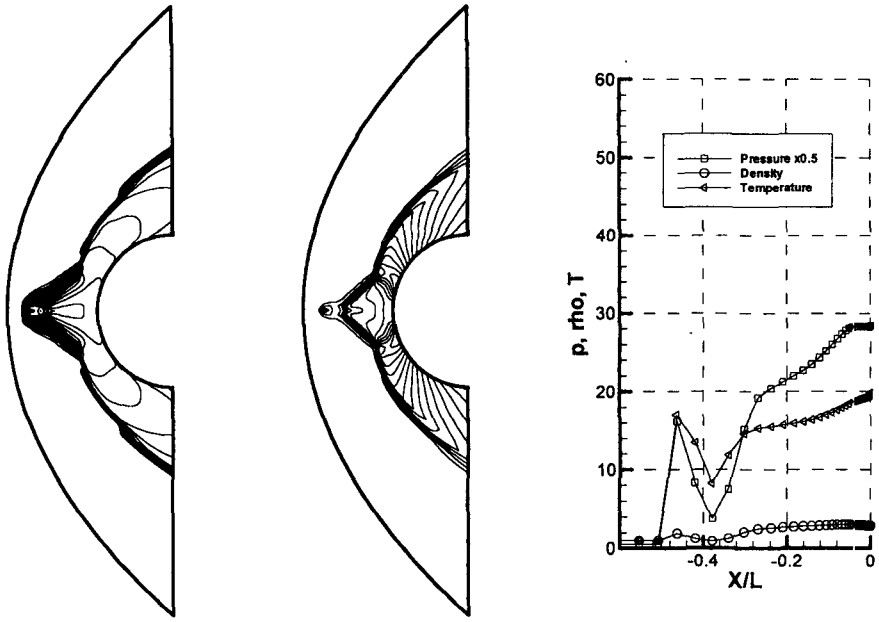

(a) (b) (c)

Figure 5. Hypersonic flow solved by the CFDS scheme at Mach 8
(a) Mach contours; (b) Pressure contours; (c) Stagnation line properties

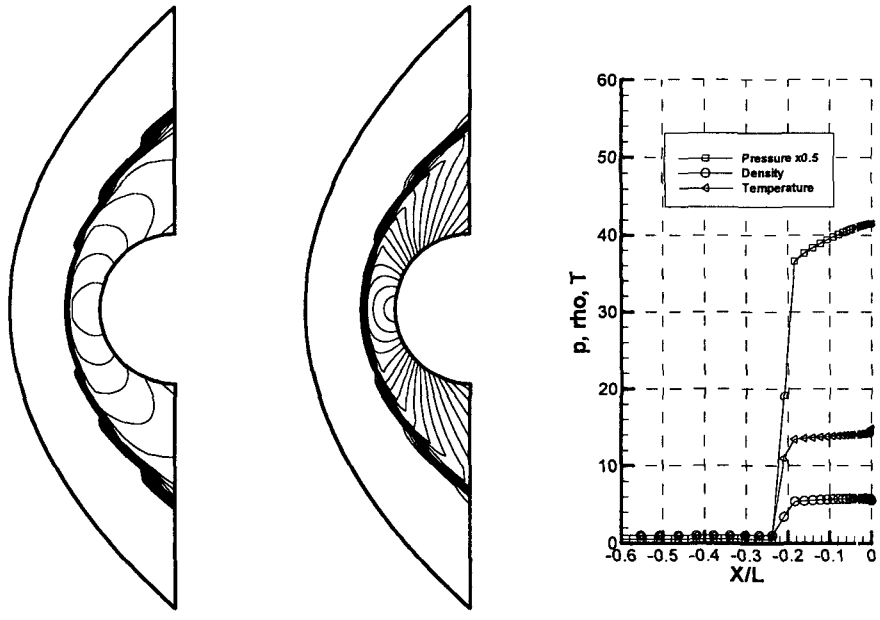

(a) (b) (c)

Figure 6. Hypersonic flow solved by the CFDS scheme at M=8(λ_1 modified)
(a) Mach contours; (b) Pressure contours; (c) Stagnation line properties

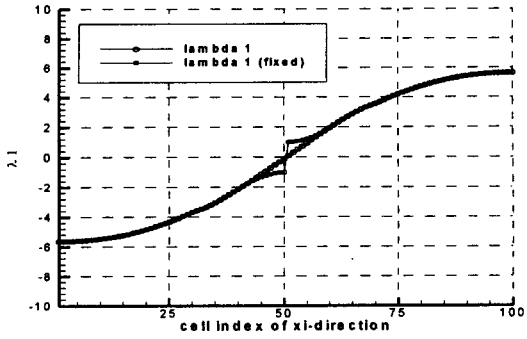

Figure 7. Comparison of λ_1 and modified λ_1

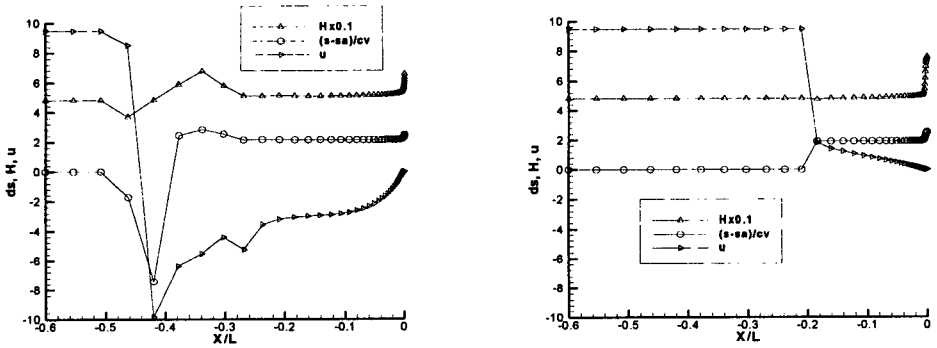

(a) (b)

Figure 8. Stagnation line properties between (a) λ_1 unmodified and (b) λ_1 modified cases.

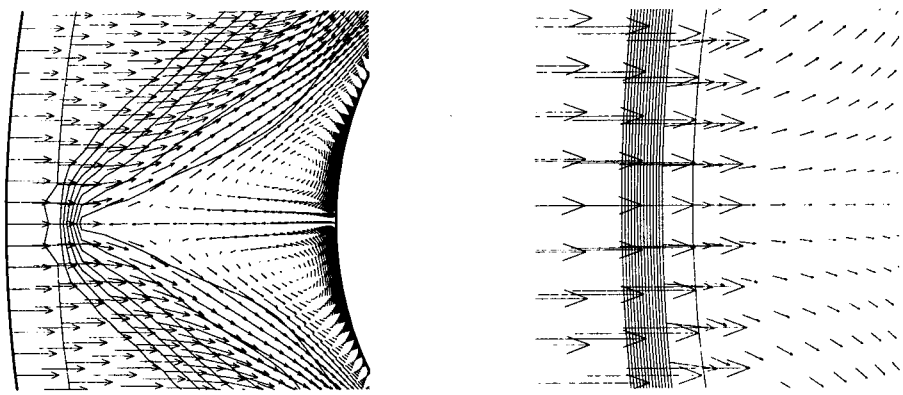

Figure 9. Velocity vectors with carbuncle(left) and w/o carbuncle(right)